J Mater Sci: Mater Electron (2017) 28:6889–6896
DOI 10.1007/s10854-017-6389-5

Preparation and characteristics study of $CuAlO_2$/Si heterojunction photodetector by pulsed laser deposition

Raid A. Ismail[1] · Fareed F. Rashid[2] · Mays S. Tariq[2]

Received: 3 December 2016 / Accepted: 13 January 2017 / Published online: 27 January 2017
© Springer Science+Business Media New York 2017

Abstract P-type copper aluminate $CuAlO_2$ thin film was deposited on glass and silicon substrates by using pulsed laser deposition technique to fabricate $CuAlO_2$ heterojunction photodetector without using any post-deposition annealing. The structural, optical and electrical properties of $CuAlO_2$ film were investigated. X-ray diffraction XRD pattern showed that the diffraction peaks are assigned to crystalline $CuAlO_2$ of rhombohedral crystal structure. UV–Vis sprctrophotometeric measurement showed that average optical transmission of 80% can be reached and the optical direct and indirect band gap values were found to be 3.6 and 2.1 eV, respectively. The photoluminescence PL investigation showed the emitting peak is centered at 390 nm corresponds to 3.52 eV, which is close to the optical band gap. Scanning electron microscopy SEM investigation revealed that the film consists of some of agglomerated particles having size in the range of 75 nm −1 µm. EDX analysis shows that the deposited film has small-off stoichiometry .The electrical and photoresponse properties of anisotype p-$CuAlO_2$/n-Si and isotype p-$CuAlO_2$/p-Si heterojunction photodetectors fabricated without using buffer layer were measured and analyzed. The heterojunctions exhibited good rectifying characteristics. The spectral response of p-$CuAlO_2$/n-Si photodetector showed maximum value of responsivity approaching 541 mA/W corresponding quantum efficiency of 90% at750nm under 2.5 V bias voltage.

✉ Raid A. Ismail
raidismail@yahoo.com

[1] Department of Applied Science, University of Technology, Baghdad, Iraq

[2] Department of Laser and Optoelectronics Engineering, University of Technology, Baghdad, Iraq

1 Introduction

P-type transparent conducting oxides TCOs have attracted attention in the field of transparent optoelectronics devices [1, 2]. Copper aluminum oxide $CuAlO_2$ thin film of optical energy gap of 3.5 eV at room temperature is one of the promising TCOs which have been studied extensively due to their high electrical conductivity and optical transmittance in visible region [3, 4].Improvement the properties of $CuAlO_2$ films via doping divalent cation have been reported [5, 6]. Various techniques were adopted to synthesis $CuAlO_2$ films including sol–gel, wet oxidation, DC sputtering, chemical vapor deposition, hydrothermal, spray pyrolysis and pulsed laser deposition [7–11] .It is reported that the deposition methods affecting the film characteristics. Few data were reported on formation of the heterostructure between $CuAlO_2$ and Si. Dong et al. [12] study the characteristics of P-$CuAlO_2$/n-Si heterostructure prepared by radio –frequency magnetron sputtering. Suzhen et al. [13] study the electrical properties of P-$CuAlO_2$/(n-,p-) Si heterostructure synthesised by chemical solution technique, they revealed that p-$CuAlO_2$/n-Si structure has a rectifying ratio of ~35 within the applied voltages of −3.0 to +3.0 V, while the p-$CuAlO_2$/p-Si structure exhibits Schottky diode-like characteristics. Up to best of our knowledge no data have been reported on fabricating of $CuAlO_2$/Si heterojunction by laser deposition technique. Here we have reported the first study on preparation and characterization of p-$CuAlO_2$/n-Si and p-$CuAlO_2$/p-Si heterostructure photodetectors by pulsed laser deposition PLD technique.

Table 1 The main specification of laser used in this study

Laser model	Q-switched Nd:YAG laser
Laser wavelength	532 nm
Pulse energy	(100–1000) mJ
Pulse duration	9 ns
Cooling method	Inner circulation of water for cooling
Power supply	220 V
Repetition frequency	(1–6) Hz

2 Experimental details

The PLD system was used to deposit $CuAlO_2$ thin films consisting of vacuum chamber with base pressure down ABCD mbar and Q-switched Nd:YAG laser, the specifications of laser are listed in Table 1. Halogen lamps were used for substrate heating. Single crystalline n-type and p-type (100) wafers having electrical resistivity of 1–3 ABCD cm and cleaned glass were used as substrates, the substrate temperature of these substrates was maintained at 200 °C during deposition process. The Laser beam was focused on rotating sintered $CuAlO_2$ pellet to a spot diameter 1.5 mm using positive lens of a 5 cm at an incident angle of 45°. Preparation of the pellet was accomplished by mixing of high purity CuO (10 g weight) powder and Al_2O_3 (7 g weight) and pressed using hydraulic press and finally, the pellet was sintered at 1100 °C using controlled furnace .The laser fluence used in this study (10 J/cm^2) was based on the optimum value reported in ref [14].After deposition of $CuAlO_2$ film, X-ray diffractometer (Shimadzu - XRD6000, Shimadzu Company /Japan) was used to investigate the structure of the $CuAlO_2$ film .The surface structure of the deposited film was investigated using scanning electron microscopy SEM (T-scan Vega III Czech).The optical transmittance of the film deposited on glass substrate was measured by using double beam UV–Vis spectrophotometer in the spectral range of 300–900 nm.The film morphology was investigated using atomic force microscopy (model AA3000) Fourier transformation infrared spectroscopy FT-IR (Shimadzu IR Affinity–1) was used to examine the chemical composition of $CuAlO_2$ film. Hall measurement was employed to investigate the conductivity type and to measure the mobility and electrical resistivity of the deposited film. In order to investigate the figures of merit of the $CuAlO_2$/n-Si heterojunction photodetector, ohmic contacts were made on $CuAlO_2$ film and silicon substrate by depositing high purity Cu and In films, respectively, using thermal resistive technique at pressure $<10^{-6}$ torr through square mask. After deposition of ohmic contacts, the sample was annealed at 400 °C for 3 min under vacuum to improve the contact resistance. The photodetector sensitive area was adjusted to be ~1 cm^2. Figure 1 shows the schematic diagram of $CuAlO_2$/Si heterostructure photodetector, no buffer layer has been used between $CuAlO_2$ film and silicon .The current–voltage of heterojunction photodetectors under dark and illumination conditions have been investigated .The photocurrent was measured as function of light intensity, a silicon power meter was used to measure the light intensity.

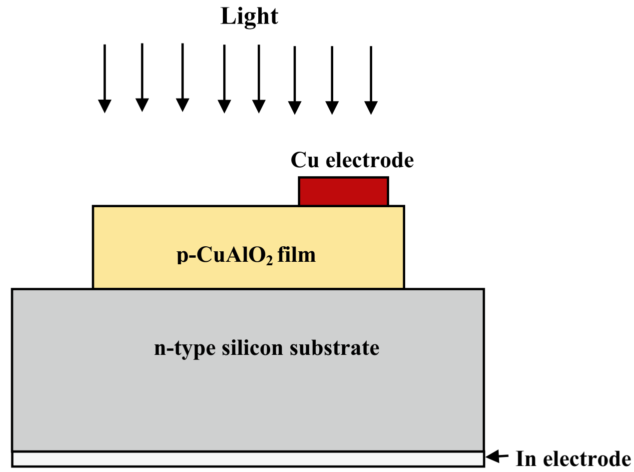

Fig. 1 Cross-sectional view diagram of P-$CuAlO_2$/n-Si heterostructure photodetector

The spectral responsivity of the photodetectors was measured with aid of calibrated monochromator. All above measurements were carried out at room temperature.

3 Results and discussion

Figure 2 shows XRD of $CuAlO_2$ film deposited on glass substrate, two diffraction peaks located at 2θ = 31.55°, 236.6° and 37.7° 2corresponding to (006), (101) and (012) planes, respectively. These peaks are indexed to structure crystalline $CuAlO_2$ with rhombohedral crystal (JCPD PDF #35-1401) [15] .It is noticed the film has poor crystalinity due to probability of decomposition of $CuAlO_2$ film which weakened the film crystalinity [6] and/or due to small off-stoichiometry .

The SEM micrograph of $CuAlO_2$ film deposited on glass substrate is shown in Fig. 3, it is clearly seen that the film is smooth and covered with some of white and grey large particles dispersed on the film surface with sizes in the range ~(75 nm–1 μm) .The large grains are ejected from the pellet formed by condensed vapor from the plume. The Particulate formation is probably due to expulsion of superheated subsurface melted target material when some of the material vaporizes. SEM

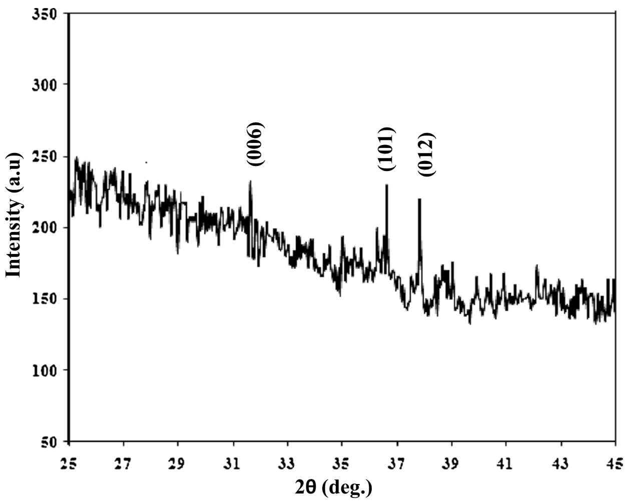

Fig. 2 XRD pattern of $CuAlO_2$ film

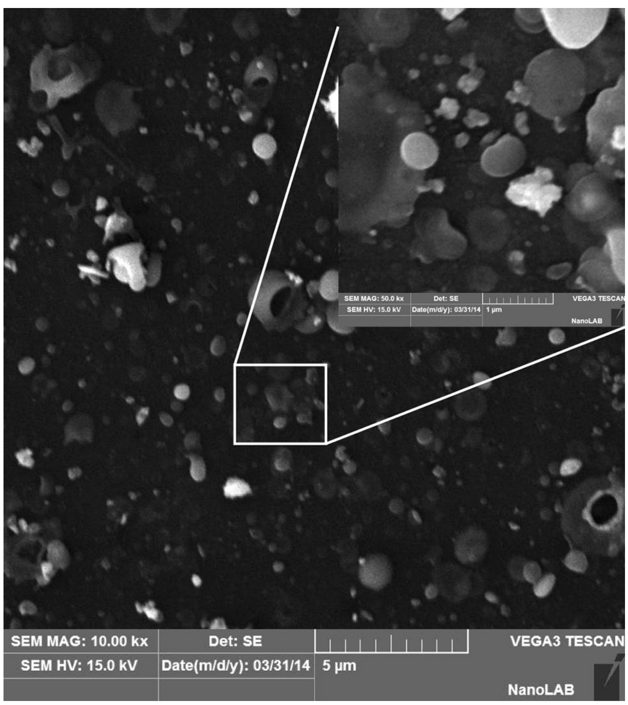

Fig. 3 SEM image of $CuAlO_2$ film surface. Inset is the magnified SEM

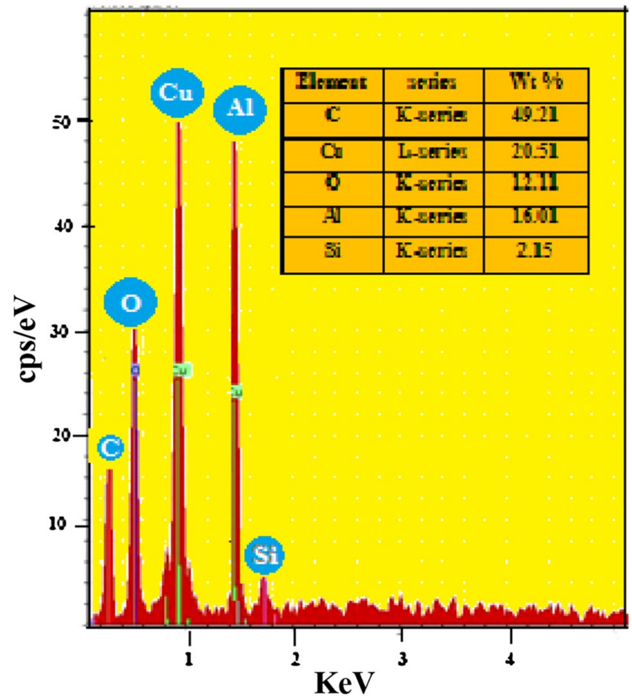

Fig. 4 EDX spectrum of $CuAlO_2$ film

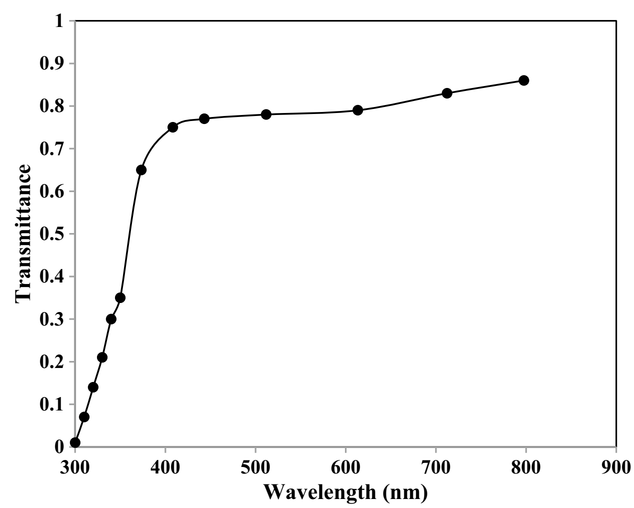

Fig. 5 Optical transmittance of $CuAlO_2$ film deposited on glass

investigation confirms that neither micro-cracks nor holes and pits were noticed .EDX spectrum as shown in Fig. 4 confirms presence of peaks related to Si, Al, O, Cu, and C. The existence of each C and Si peaks could be arose from the substrate .The atomic ratio of Cu:Al:O was about 1:1.2:1.7 indicating the formation of small off- stoichiometry $CuAl_{1.2}O_{1.7}$ phase which is in good agreement with XRD result.

Figure 5 shows the optical transmittance spectrum of $CuAlO_2$ film of 250 nm thick deposited on glass substrate. It clearly seen from this figure that the film has an average optical transmittance of ~80%.

The optical band gap E_g of the films was calculated from Tauc law:

$$\alpha h\nu = A(h\upsilon - E_g)^n \tag{1}$$

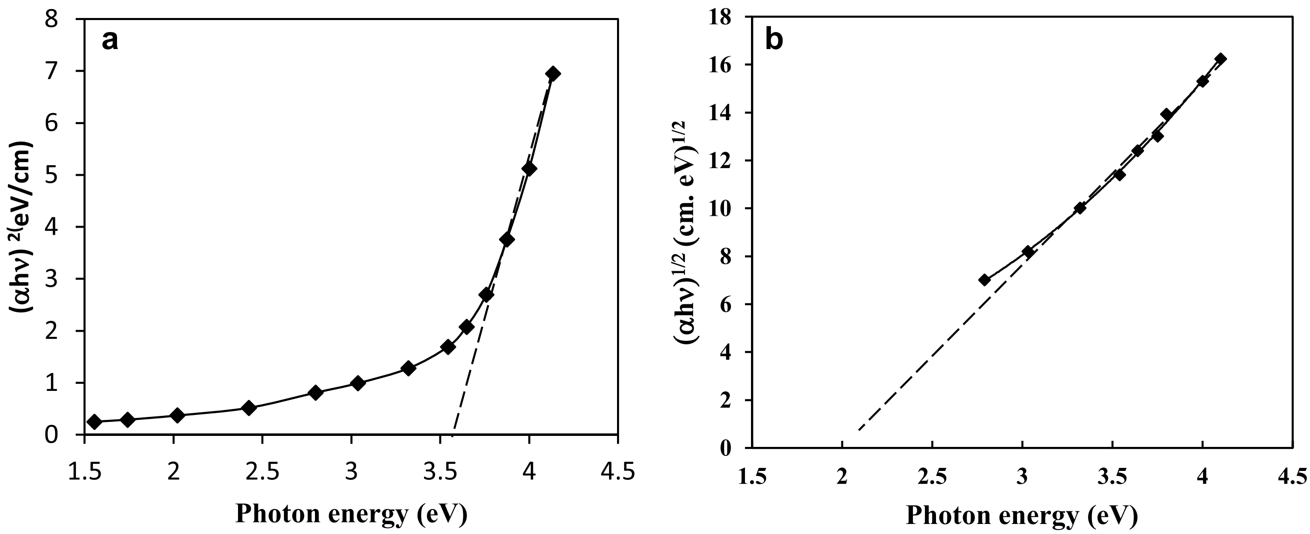

Fig. 6 Plot of direct allowed transition (**a**) and indirect transition of film (**b**)

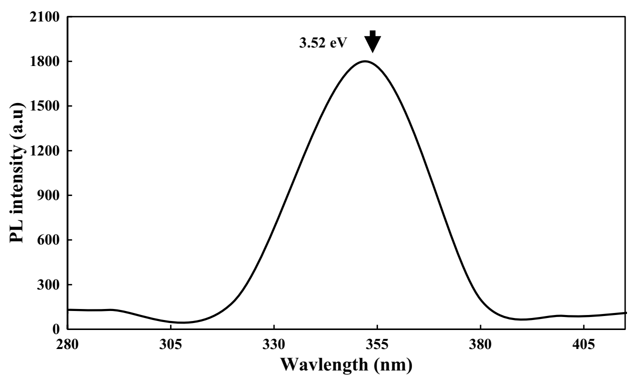

Fig. 7 PL spectrum of $CuAlO_2$ film

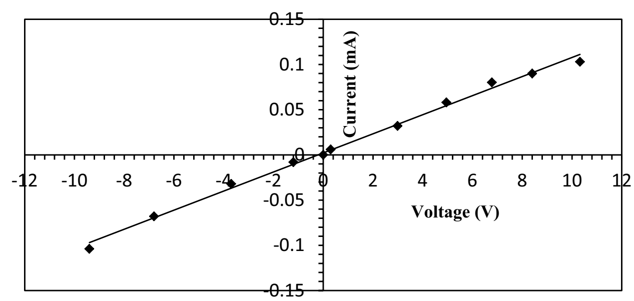

Fig. 8 Room temperature I–V characteristic of Cu-$CuAlO_2$ contact

where α is the film absorption coefficient, hν is photon energy, A is a constant, h is the Plank constant, n is the exponent that gives the type of band transition. For direct allowed, $n=1/2$, for indirect allowed transition, $n=2$, and for direct forbidden, $n=3/2$. The direct energy gap was determined from the $(\alpha h\nu)^2$ versus $h\upsilon$ plot by extrapolating the straight line of the curve to the$h\upsilon = 0$ points as shown in Fig. 6-a, while the indirect band gap was obtained from $(\alpha h\nu)^{\frac{1}{2}}$ versus $h\upsilon$ plot (Fig. 6-b).The values of direct and indirect band gap of the $CuAlO_2$ film were around 3.6 eV and 2.1 eV, respectively, which in good agreement with reported results [6, 15].

Figure 7shows the room temperature PL of $CuAlO_2$ film, the emession peak is centered at 390 nm corresponds to 3.52 eV which is very close to direct optical energy gap calculated from optical absorption, indicating that the emission with the excitation wavelength of 365 nm arise from the $CuAlO_2$ near-band-edge transition [16, 17]. No additional emitting peaks were observed in spectrum. Figure 8 displays the I–V characteristics of Cu/p-$CuAlO_2$ contact. The contact exhibits the linear I-V over wide range of applied voltage (−10 to 10 V) indicating formation of good ohmic contact .This can be attributed to the thermal annealing that resulted in formation of metal deficiency layer near $CuAlO_2$ surface and consequently this increased the number of vacancies and in turns increase the surface carrier concentration [18].

Electrical measurement revealed that Hall coefficient was found + 59 cm^3/C indicating the conduction nature of the deposited $CuAlO_2$ film was p-type .The origin of p-type conductivity of $CuAlO_2$ might be ascribed to excess of oxygen within crystallite site according to the following defect equilibrium equation [19]:

$$O_2(g) = 2O_O^x + V_{Cu}^- + V_{Al}^{-3} + 4h^+$$

where O_O is the lattice oxygen, V_{Cu} is the Cu vacancy,V_{Al} is the Al vacancy, and h represents the hole, respectively. The x, − and + superscripts refer to effective neutral, negative and positive charge states, respectively.The value of electrical resistivity and mobility of the film at room temperature were 1.5×10^2 Ω cm and 2.9 cm^2 V^{-1} s^{-1}, respectively. The value of mobility was comparable to that of film prepared by spin-on technique [20]. The morphology and surface roughness of the film was determined from AFM investigation. Figure 9 shows two-dimensional 2D and 3D AFM images (1.5×1.5 µm scanned area) and grain size distribution plot of the deposited film. The AFM image showed that grains are vertically oriented and have different sizes due to coalescence of small grains.

The surface root mean square roughness RMS of the film was found to be 8.18 nm.The grain size distribution chart confirms that the grains have different sizes. The average grain size has been estimated using software and was around 80 nm. Figure 10 displays I–V characteristics under forward and reverse directions of anisotype p-$CuAlO_2$/n-Si and p-$CuAlO_2$/p-Si heterojunctions at dark condition, the rectification factor was found to be around for 18 $CuAlO_2$/n-Si, while for isotype p-$CuAlO_2$/p-Si, the rectification factor was around 9 within applied voltage

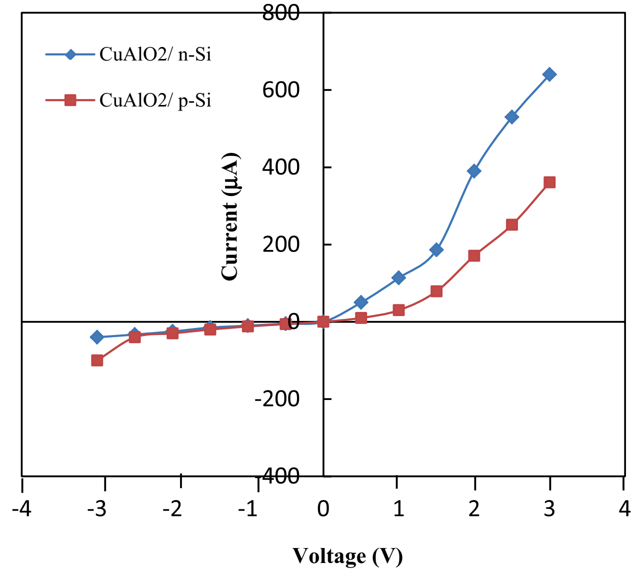

Fig. 10 Dark I–V characteristics of $CuAlO_2$/Si heterojunction

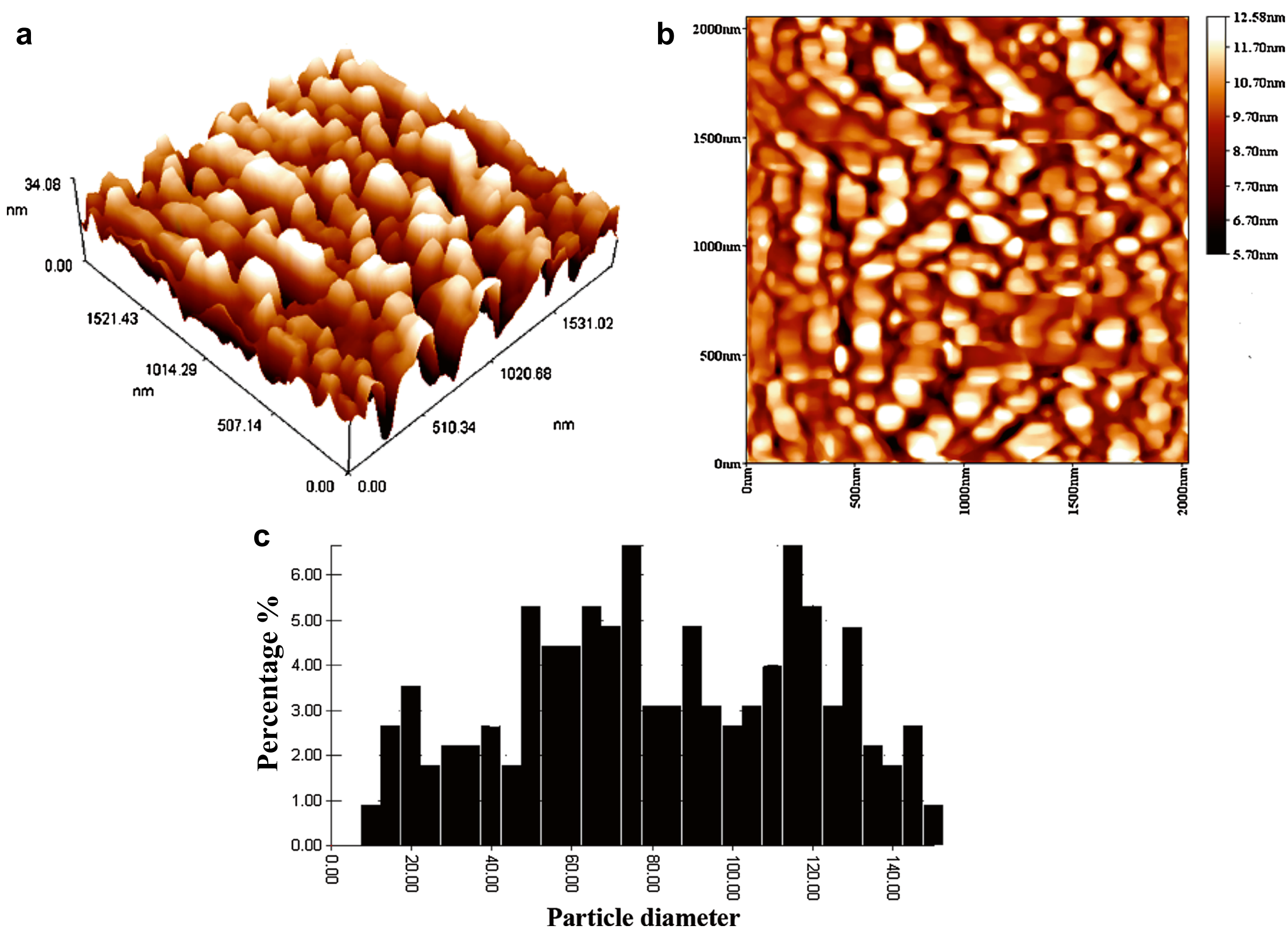

Fig. 9 AFM image of the film **a** 3D, **b** 2D and **c** grain size distribution plot

−2.5 V to +2.5 V. The forward current I_f increases with applied voltage in both heterojunction and it clearly seen that its value for $CuAlO_2$/n-Si was larger than that of $CuAlO_2$/p-Si.The current transportation for p-$CuAlO_2$/p-Si heterojunction is representing as Schottky barrier devices, the turn-on voltage was estimated to be as small as 1.2 V which is in good agreement with the results reported for $CuAlO_2$/p-Si prepared by chemical solution deposition [13] .The ideality factor of the heterojunction β was calculated from the following equation and was found as 2.5 and 4 for $CuAlO_2$/n-Si and $CuAlO_2$/p-Si heterojunctions, respectively, indicating the domination of the current transport by recombination process.

$$\beta = \frac{q}{Kt}\frac{\Delta V}{\Delta ln\frac{I_f}{I_s}} \tag{2}$$

The large value of ideality factor indicating can attributed to structural defects originated from interfacial defects and surface states as well as the lattice mismatch lattice between $CuAlO_2$ film and Si substrate [13]. The reverse current was found to be near voltage independent for bias voltage V_{bias} ˂3 V, but at 3 V starting of soft breakdown was noticed for CuAlO/p-Si heterojunction. The illuminated I-V characteristic of $CuAlO_2$/n-Si and $CuAlO_2$/p-Si heterojunctions under reverse direction is given in Fig. 11.

The on/off ratio (photocurrent to dark current ratio) of $CuAlO_2$/n-Si heterojunction (Fig. 11-a) was calculated and found its maximum value was around 95 at light intensity and bias voltage of 160 mW/cm^2 and 2.5 V, respectively, while it was 17 for $CuAlO_2$/p-Si heterojunction (Fig. 11-b). This result can explained on the basis that the $CuAlO_2$/p-Si has larger dark current and smaller photocurrent which probably resulted from small space charge region formed in this contact compared to large deletion region in the case of $CuAlO_2$/n-Si heterojunction. It is obvious from this figure that increasing the light intensity leads to increase the photocurrent due to generation of e-h pairs arise from absorption of the light in the depletion region and/or diffusion length .On the other hand, no saturation in photocurrent was observed at large light intensity indicating the good linearity characteristics of photodetector as shown in Fig. 12

The spectral responsivity R_λ plot of heterojunction at −2.5 V bias is given in Fig. 13. The responsivity was calculated from the following equation.

$$R_\lambda = \frac{I_{ph}}{P} \tag{3}$$

where I_{ph} is photocurrent at specific wavelength and P is the incident light power at specific wavelength. It is clearly that peaks of response of these two heterojunctions was located at 750 nm (due to absorption edge of

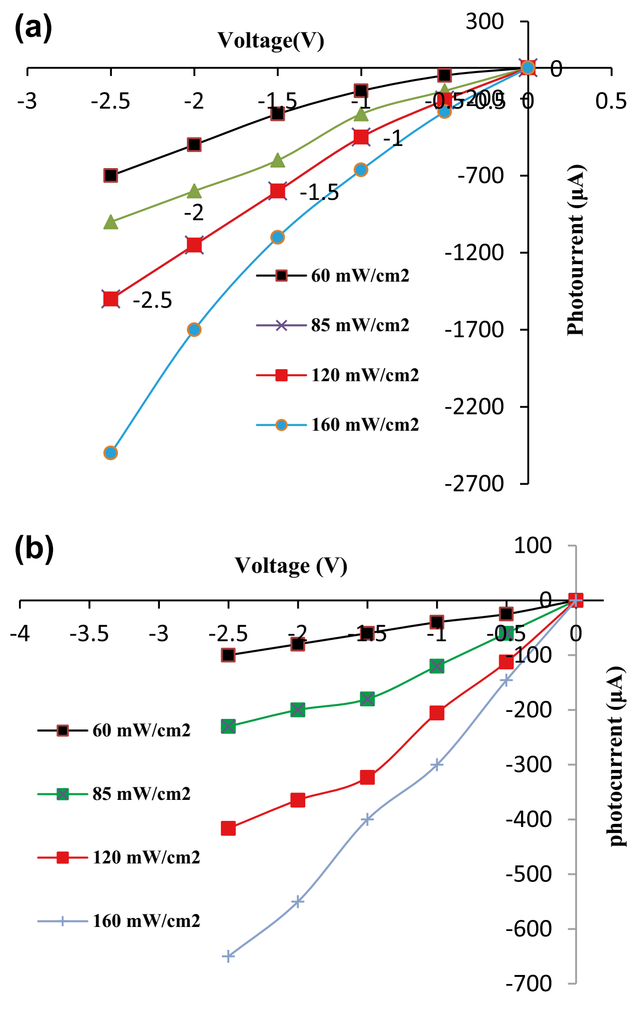

Fig. 11 Illuminated I-V characteristics of $CuAlO_2$/n-Si heterojunction (**a**) and $CuAlO_2$/p-Si heterojunction (**b**) at different light intensities

underlaying substrate) with flat response of 400-750nm. We have noticed a shoulder at short wavelength in the spectral response plot which can attributed to the absorption edge of $CuAlO_2$ film. The maximum responsivity of heterojunction was 541 mA/W and 400 mA/W at 750 nm for $CuAlO_2$/n-Si and $CuAlO_2$/p-Si, respectively. The responsivity of $CuAlO_2$/p-Si (isotype) at peak response was lower than that for $CuAlO_2$/n-Si (anisotype) heterojunction because it has small depletion layer width compared to that for $CuAlO_2$/n-Si [13, 21]. The large value of sensitivity makes these photodetectors competitive to other high sensitivity wide band gap—silicon based heterojunction photodetectors [22, 23]. The maximum quantum efficiency of $CuAlO_2$/n-Si photodetector was estimated and it founds about 90% and it was 66% for $CuAlO_2$/p-Si at 750 nm as shown in Fig. 13.This figure confirms that no effect of substrate conductivity type (-p or -n type silicon) on the location of peak of response of the photodetectors.

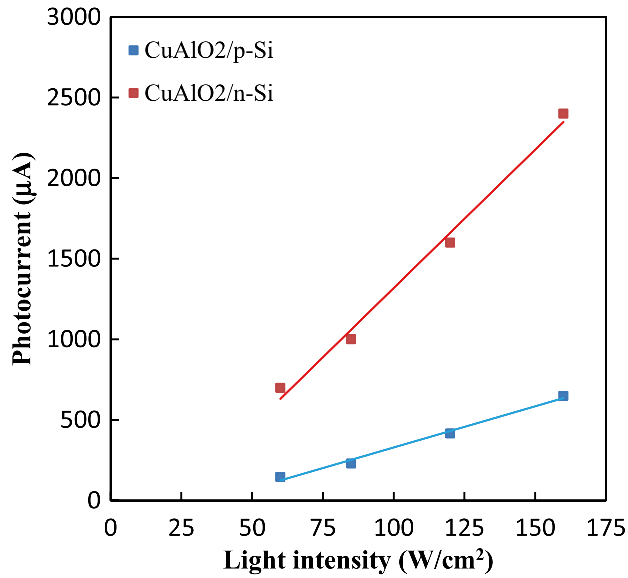

Fig. 12 Linearity characteristics of $CuAlO_2$/n-Si and $CuAlO_2$/p-Si heterojunctions photodetector

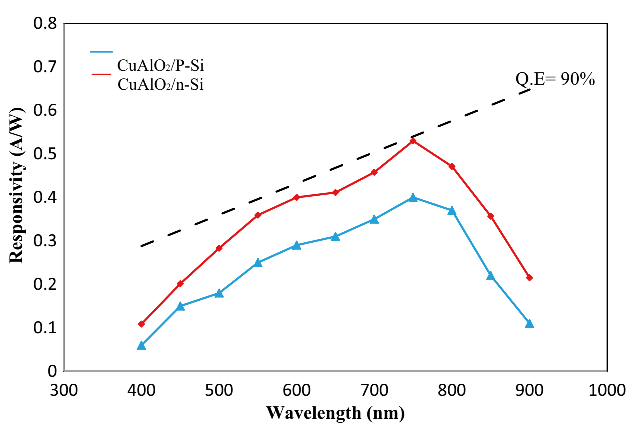

Fig. 13 Spectral responsivity plot of $CuAlO_2$/n-Si and $CuAlO_2$/p-Si heterojunctions

Figure 14 displays the specific detectivity D* of photodetectors versus wavelength at 2.5 V bias, the peak detectivity of the synthesised photodetector is approximately 2×10^{12} W^{-1} cm Hz (Jones) at 800 nm for anisotype heterojunction, the calculation of D* based on assumption that the shot noise I_s is the dominant source of the noise current I_n. The value of D* of $CuAlO_2$/p-Si was smaller than that of $CuAlO_2$/n-Si due large leakage current and lower responsivity of the former. Decreasing the D* after 800 nm is due to recombination effect. The corresponding NEP was calculated from the following equation which found to be 5×10^{-13} W.

$$NEP = \frac{(A\Delta f)^{0.5}}{D^*} = \frac{A^{0.5}R}{I_n} \tag{4}$$

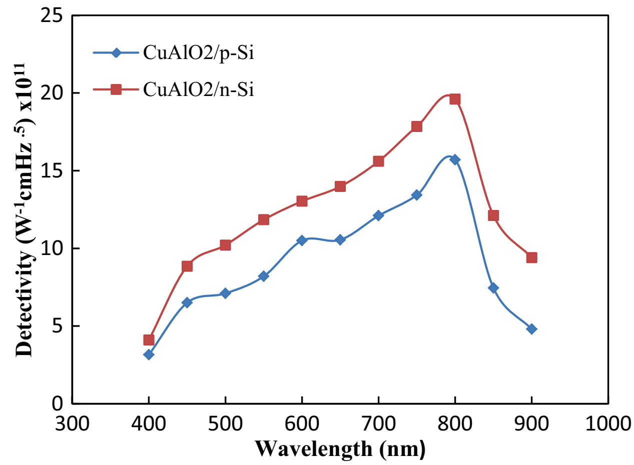

Fig. 14 Specific detectivity as function of wavelength for $CuAlO_2$/n-Si and $CuAlO_2$/n-Si heterojunctions

$$I_n = I_s = (2qI_d\Delta f)^{o.5} \tag{5}$$

where A is the sensitive area of photodetector and Δf is the bandwidth and I_d is the dark current.

4 Conclusions

P-$CuAlO_2$ thin film was deposited on glass and silicon substrates by pulsed laser deposition technique. XRD results showed that the deposited $CuAlO_2$ was polycrystalline in nature with rhombohedral crystal structure. The film has an average optical transmittance of 80% and the optical energy gap of the film was 3.6 eV for direct transition and 2.1 eV for indirect transition. PL data of the film revealed that the emession peak is centered at 390 nm corresponds to 3.52 eV. The p-$CuAlO_2$/n-Si heterostructure exhibited rectification characteristics better than $CuAlO_2$/p-Si heterostructure, the current transport of $CuAlO_2$/p-Si contact is similar to the Schottky diode. The $CuAlO_2$/n-Si photodetector figures of merit were better than that of $CuAlO_2$/p-Si photodetector, both photodetectors have broad band spectral response of (400–900) nm with peak peaks of response located at 550 and 750 nm .The responsivity of $CuAlO_2$/n-Si at 550 nm was 359 mA/W and was 532 mA/W at 750, while the responsivity of $CuAlO_2$/n-Si at 550 nm was 359 mA/W and was 532 mA/W at 750,. The high value of responsivity of synthesised photodetector suggesting that the technique used here was encouraging and promising for fabricating simple and cost- effective high performance visible photodetector.

References

1. R. Ismail, O. Razzaq, Solar Energy Mater. Solar Cells **91**, 903 (2007)
2. M. Chowdhury, A. Kunti, S. Sharma, M. Gupta, R. Chaudhary, Eur. Phys. J. Appl. Phys. **67**, 10302 (2014)
3. R. Ismail, D. Raouf, D.F. Raouf, J. Optoelectron, Adv. Mater. **8**, 1443 (2006)
4. E. Ko, J. Choi, H. Jung, S. Choi, C. Kim, J. Nanosci. Nanotechnol. **16**, 1934 (2016)
5. J. Pan, W. Lan, H. Liu, Y. Shen, B. Feng, X. Zhang, E. Xie, J. Mater. Sci **25**, 4004 (2014)
6. G. Dong, M. Zhang, W. Lan, P. Dong, H. Yan, Vacuum **82**, 1321 (2008)
7. N. Benreguia, A. Barnabé M, Trari. J. Sol-Gel. Sci. Technol. **75**, 670 (2015)
8. D. Kim, S. Park, E. Jeong, H. Lee, S. Choi. Thin Solid Films **515**, 5103 (2007)
9. D. Shahriari, A. Barnabè, T. Mason, K. Poeppelmeier, Inorg. Chem. **40**, 5734 (2001)
10. V. Saravanakannan, T. Radhakrishnan, Surf. Eng. **32**, 21 (2016)
11. H. Yanagi, S. Inoue, K. Ueda, H. Kawazoe, H. Hosono, N. Hamada, J Appl. Phys. **88**, 4159 (2000)
12. G. Dong, M. Zhang, W. Lan, P. Dong, X. Zhao, H. Yan, J. Mater. Sci. **20**, 193 (2009)
13. W. Suzhen, D. Zanhong, D. Weiwei, S. Jingzhen, F. Xiaodong, J. Semicond. **35**, 043001 (2014)
14. M. Tariq, Preparation and characterization of $CuAlO_2$/Si Photodetector by pulsed laser deposition, M. Sc thesis, University of Technology, Iraq (2014)
15. A. Banerjee, R. Maity, K. Chattopadhyay, Thin Solid Films **440**, 5 (2003)
16. Y. Liua, Y. Gonga, N. Mellotta, B. Wanga, H. Yeb, Y. Wu, Sci. Technol. Adv. Mater. **17**, 200 (2016)
17. D. Byrne, A. Cowley, N. Bennettc, E. McGlynna, J. Mater. Chem. C **2**, 7859 (2014)
18. J. Lim, K. Kim, D. Hwang, H. Kim, J. Oh, S. Park, J. Electrochem. Soc. **152**, G179 (2005)
19. P. Kofstad, Nonstoichiometry, *Diffusion, and Electrical Conductivity in Binary Metal Oxides* (Wiley, New York, 1972), p. 19
20. S. Gao, Y. Zhao, P. Gou, N. Chen, Y. Xie, Nanotechnology **14**, 538 (2003)
21. R. Ismail, K. Yahya, O. Abdulrazaq, Surf. Rev. Lett. **12**, 299 (2005)
22. Y Hassa, Sh. Kakil ,J. Mater. Sci. **20**, 193 (2009), **26**, 6092 (2015)
23. R. Ismail, S. Al-Jawad, N. Hussein, Appl. Phys. A **117**, 1977 (2014)